Novel Hybrid Wireless-Power Line Video Sensor Networks with Distributed Cross-Layer Optimization

Kainan Zhu*, Xu Zhu*, Yufei Jiang† and Weiqiang Xu‡
*Department of Electrical Engineering and Electronics, The University of Liverpool, Liverpool, UK
Email: {K.zhu3, Xuzhu}@liverpool.ac.uk
†School of Electronic and Information Engineering, Harbin Institute of Technology (Shenzhen), Shenzhen, P. R. China
Email: Jiangyufei@hit.edu.cn
‡School of Information Science and Technology, Zhejiang Sci-Tech University, Hangzhou, P. R. China
Email: wqxu@zstu.edu.cn

***Abstract*—A hybrid video sensor network, which comprises the power line nodes and the wireless nodes is proposed in this paper to extend the network lifetime. We take the video encoding rate, node energy consumption, channel access control, and link rate allocation into account jointly to formulate the problem. We develop a fully distributed algorithm which achieves very close performance compared to the centralized algorithm, while saving significant communication overhead required by the centralized algorithm. By extensive simulations, we show that the network lifetime is extended by 35% and 42% in the proposed hybrid video sensor network, compared to pure wireless video sensor networks with different network configurations.**

I. Introduction

Wireless video sensor networks (WVSNs) are tasked to perform video capturing and processing and to forward the processed video content to a remote control unit (or the sink node) via wireless channels for further data analysis and decision making [1]. Unlike standard mains powered WVSNs [2], battery-operated WVSNs may be widely adopted in fields such as impromptu surveillance installation, home security and in-home elder care due to the advantages of discreet and unobtrusive installation and removal. In addition, battery-operated WVSNs are immune to power outage. Several battery powered wireless cameras used for the purpose such as home security, pet monitoring and assisted living have been produced and marketed [3] [4].

In typical scenarios, battery-powered WVSNs are supposed to offer high-quality video and at the mean time, to support high data rates, which results in a significant power consumption at the video sensor. Although battery replacement may be feasible in certain scenarios, replacing battery for a large number of video sensors regularly is cumbersome. Therefore, maintaining a low energy consumption level is critical for WVSNs. In the home or smart building environment, one ubiquitous infrastructure that can potentially serve as the data communication medium is the power line (PL) cables. Since the wireless video sensors have the advantage of flexibility that PL sensors lack (PL sensors have to be attached to the power sockets) while unlike wireless video sensors, in which energy is a scarce resource and wireless links often exhibit blind spot problems, the PL sensors potentially have unlimited energy supply and can utilize power line communication (PLC). This leads to the idea to prolong the network lifetime by using the hybrid wireless and PL video sensor networks.

Extensive research has been conducted focusing on network lifetime maximization problems of traditional wireless sensor networks [5] [6]. Also, in our previous work [7], we derived the globally optimal solution in a closed-form expression for network lifetime maximization problem in a hybrid sensor network. However, the energy consumption model adopted in these works is based on conventional sensor networks, in which the power consumption due to data processing is often neglected due to the low complexity of the processing. In contrast, in video sensor networks, the data is compressed and efficient video compression algorithm consumes high power consumption.

In [8], the authors developed a distributed algorithm to maximize the network lifetime of WVSNs [1]. However, there is no limit on the channel capacity. The authors in [9] studied the optimization tradeoff between video distortion and network lifetime by jointly considering source/channel rate adaptation and network coding for an energy constrained WVSNs. A distributed algorithm is developed in [10] to achieve the tradeoff between video distortion and network lifetime by joint design of coding and routing optimization in WVSNs with correlated sources. In [11], the authors studied the placement design of motion sensor and camera for network lifetime maximization, in which the cameras are activated whenever motion is detected.

In this work, a hybrid video sensor network (HVSN) which comprises battery-powered wireless sensor nodes and PL sensor nodes is proposed for network lifetime maximization. Our work differs with existing work in the following aspects. Firstly, to the best of the authors' knowledge, this is the first reported study to investigate video sensor networks with hybrid power sources and hybrid communication schemes. The proposed HVSN utilizes the flexibility of wireless nodes while PL nodes are used to extend the network lifetime. Secondly, we jointly study the design of source encoding rate, node energy consumption, channel access control, along with link rate allocation for hybrid network lifetime maximization. The joint design achieves much better performance than separate optimization while at comparable complexity. Thirdly, a distributed algorithm is proposed for the hybrid network lifetime maximization problem, which was not presented in the literature. The distributed algorithm divides the computational burden among all nodes with much lower communication overhead. The solution obtained is very close to the one

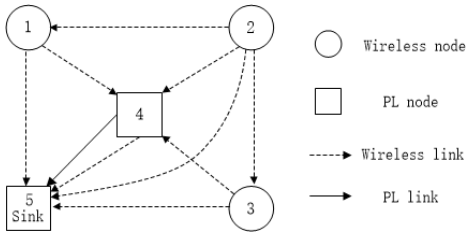

Fig. 1. Topology of an example HVSN

obtained from the centralized algorithm.

We organize the remainder of this paper as follows. Section II introduces the system model. The optimization problem is outlined in section III. In section IV, a distributed algorithm is proposed. The simulation results are presented and analysed in section V. Finally, section VI concludes the paper.

II. System Model

We study a HVSN that includes both wireless video sensor nodes and PL sensor nodes, as depicted in Fig. 1. The wireless video sensor nodes are placed high above the room and perform video capturing, encoding, and routing. The power line sensor nodes simply perform as relay nodes to help to forward the video content collected by the wireless nodes to the sink node, which is the remote control unit acting as destinations of the HVSN. The PL nodes are assumed to be mounted with wireless transceivers, such that they can communicate with other nodes via wireless links.

The PL nodes set is labeled as $\mathbb{P} = \{1, ..., |P|\}$ and the wireless nodes set is denoted by $\mathbb{W} = \{1, ..., |W|\}$. S is used to denote the single sink node in the network. We define L_p as the count of the PL links and L_w as the count of the wireless links. We denote $\mathcal{L}_p$ and $\mathcal{L}_w$ as the set of all the PL and wireless links, respectively, in which $\mathcal{L}_p = \{1, ..., L_p\}$ and $\mathcal{L}_w = \{1, ..., L_w\}$. Also, we denote $l_p \in \mathcal{L}_p$ as the index to the l-th PL link and $l_w \in \mathcal{L}_w$ as the index to the l-th wireless link. $\mathcal{L} = \mathcal{L}_w \bigcup \mathcal{L}_p$ represents the set of all links and $l \in \mathcal{L}$ denotes the l-th link, which originates from node i to is received by node j and is represented by (i, j). We denote $\mathcal{I}(i)$ and $\mathcal{O}(i)$ respectively as the set of incoming and outgoing links at node i.

A. Video Distortion Model

Unlike traditional wireless sensor networks, the video content captured by the video sensor network is first compressed locally before being injected into the channel for transmission. The end-to-end distortion D is caused by two factors [12]: 1) transmission distortion D_t due to transmission errors and 2) source coding distortion D_c due to video compression. Generally, according to [12], the transmission and encoding distortions are uncorrelated, we have

$$D = D_c + D_t \tag{1}$$

For the distortion caused by video compression, an analytic power-rate-distortion (P-R-D) model is established in [1], which relates the encoding rate $R^{(i)}$, power consumption due to video encoding $P_c^{(i)}$, and the distortion caused by video compression $D_c^{(i)}$ for each wireless node i as

$$D_c^{(i)} = \sigma^2 e^{-\gamma \cdot R^{(i)} \cdot \left(P_c^{(i)}\right)^{2/3}} \tag{2}$$

where γ is a factor connects to the encoding efficiency, and σ^2 represents the average input variance. Apparently, a target encoding distortion is achievable by adjusting either the encoding power or the source rate.

On the other hand, for the distortion caused by transmission, it is shown in [13] that after a certain threshold of bit error rate (BER) is achieved, the video quality would not increase significantly with further decrease in BER. This indicates that, although channel conditions are rather variable, the distortion can be neglected with a proper target BER value.

B. Channel Access Model

A widely adopted medium access control (MAC) protocol in sensor networks is the contention-based MAC protocol [10]. In this paper, we use the p-persistent contention based MAC protocol. In such a protocol [10], each node i has a certain persistence probability P_i to compete for channel access. It is assumed that time is split into intervals and the transmission of the node begins at the start of each interval. If node i is ready for transmission, it picks a link $l \in \mathcal{O}(i)$ (*i.e.*, $(i, j) \in \mathcal{O}(i)$) out of all its outgoing wireless or PL links with probability q_l, and competes to access the channel with persistence probability P_i. Hence, link $l \in \mathcal{O}(i)$ has a transmission attempt probability $p_l = q_l \cdot P_i$, where $\sum_{l \in \mathcal{O}(i)} q_l = 1$. Therefore, the persistence probability is

$$P_i = \sum\nolimits_{l \in \mathcal{O}(i)} p_l \tag{3}$$

where $0 \le p_l \le 1, \forall l \in \mathcal{L}$, and $0 \le P_i \le 1, \forall i \in \mathbb{W} \bigcup \mathbb{P}$.

In continuous video acquiring applications, assuming the packet loss probability through link l is ε_l, the success probability for packet transmission can be expressed as

$$\tau_l = (1 - \varepsilon_l) \cdot p_l \cdot \prod\nolimits_{k \in N_l^I} (1 - P_k) \tag{4}$$

where N_l^I is the set of nodes whose transmissions introduces interferences to the end node of link l. For wireless links, we assume that any outgoing link of node m interferes with link (i, j) if $d_{(m,j)} < (1 + \Phi) \cdot d_{(i,j)}$, where $\Phi \ge 0$ represents the area of interference. For power line links, we assume that any outgoing link of node m interferes with link (i, j) if $\frac{G_{(i,j)} \cdot \overline{p}_{(i,j)}}{G_{(m,j)} \cdot \overline{p}_{(m,j)} + B_{(i,j)} \cdot N_0} < \gamma_{thres}$, where $G_{(i,j)}, \overline{p}_{(i,j)}$ and $B_{(i,j)}$ are the channel gain, transmission power and transmission bandwidth on link (i, j), respectively, N_0 is the noise power spectral density and γ_{thres} is a pre-defined threshold. The average throughput of link l can thus be defined as

$$c_l = C_l^0 \cdot \tau_l \tag{5}$$

where C_l^0 is the maximum rate support by the channel at link l. In addition, the information flow rate f_l on link l is limited by the link capacity, as

$$f_l \le c_l, \forall l \in \mathcal{L} \tag{6}$$

In order to obtain the maximum transmission rate C_l^0, the ITU indoor path loss model [14] is used for the wireless links, as

$$G_l = 20\cdot \log_{10}(f) + 10\cdot n\cdot \log_{10}(d_l) + Lf(n) - 28dB \quad (7)$$

where f is the transmission frequency in MHz, n is the path loss exponent, d_l is the transmission range in m and $Lf(n) = 0$ for same floor transmission. For PL links, the random PLC channel generator [15] is used to determine the channel gain, G_l.

We adopt the M-ary Quadrature Amplitude Modulation in this work. Also, assuming the noise in both links is additive white Gaussian noise with power spectral density N_l. Then, with the corresponding transmission power $\overline{p}_l$ and transmission bandwidth B_l, the instantaneous transmission rate is determined as [16]

$$C_l^0 = B_l\cdot log_2(1 + \frac{K\cdot G_l\cdot \overline{p}_l}{N_l\cdot B_l}) \quad (8)$$

where $K = -1.5/ln(5\cdot BER)$ is the maximum possible coding gain given a target bit error rate (BER), BER, for modulation schemes such as MQAM [5].

C. Flow Conservation Constraint

In this work, we assume each wireless node is tasked to capture and compress video that should be delivered to a single destination. Then the video traffic is generated with a source rate $R^{(i)}$ in each node i, which can be obtained from (2). Note that $R^{(i)} = 0$ for all PL nodes, that is, $\forall i \in \mathbb{P}$. Since the PL nodes perform as relay nodes. For the sink node, the source rate is defined as $R^{(S)} = -\sum_{i\in\mathbb{W}} R^{(i)}$. Therefore, for each node i, the following constraint holds,

$$\sum\nolimits_{l\in\mathcal{I}(i)} f_l + R^{(i)} = \sum\nolimits_{l\in\mathcal{O}(i)} f_l, \forall i \in \mathbb{W}\bigcup\mathbb{P} \quad (9)$$

where f_l is the information flow rate on link l. The flow conservation law simply states that for each node, the outgoing information flow rate should be equal to the incoming information flow rate plus the data rate generated locally.

D. Energy Consumption Model

In the HVSN, we only focus on the energy consumption of the wireless nodes since the battery capacity of these nodes limits the network lifetime. In this design, the total power consumption of a wireless node is caused by video encoding, data transmission and reception.

The power consumption due to video compression can be calculated by the P-R-D model, as in (2). According to the power consumption model widely adopted in wireless sensor networks [9, 10], the power consumption caused by transmission at wireless node i is expressed as

$$P_t^{(i)} = \sum\nolimits_{l\in\mathcal{O}(i)} (\alpha + \beta\cdot d_l^n)\cdot \frac{f_l}{\tau_l} \quad (10)$$

where f_l is the rate assigned on link l, τ_l is the probability for a successful packet transmission of link l, $\frac{f_l}{\tau_l}$ is the actual rate transmitted through link l. α denotes the energy cost of the transmit electronics, β represents a coefficient relating to the energy cost of the transmit amplifier, d_l is the transmission range of link l, and n is the path-loss exponent [16].

The data reception power consumption at node i is

$$P_r^{(i)} = c^r \cdot \sum\nolimits_{l\in\mathcal{I}(i)} \frac{f_l}{\tau_l} \quad (11)$$

where c^r is the energy consumption cost of the radio receiver and $\sum_{l\in\mathcal{I}(i)} \frac{f_l}{\tau_l}$ is the actual aggregate rate transmitted to node i.

Therefore, the overall power consumption at wireless node i can be expressed as

$$P^{(i)} = \left[\frac{1}{\gamma\cdot R^{(i)}}\cdot \ln\left(\frac{\sigma^2}{D_c^{(i)}}\right)\right]^{\frac{3}{2}} + P_t^{(i)} + P_r^{(i)} \quad (12)$$

E. Network Lifetime

We consider the network lifetime as the minimum functioning durations of all wireless nodes, which is the duration from the beginning of the network till the first wireless node running out of energy. In the HVSN, the battery capacity of each node $i \in \mathbb{W}$ is denoted as $E^{(i)}$. Therefore, the lifetime of each node i is

$$T_i = \frac{E^{(i)}}{P^{(i)}}, \forall i \in \mathbb{W} \quad (13)$$

Hence, the network lifetime is

$$T_{net} = \min_{i\in\mathbb{W}}\{T_i\} = \min_{i\in\mathbb{W}}\{\frac{E^{(i)}}{P^{(i)}}\} \quad (14)$$

III. Problem Formulation

The problem under study in this work can be described as follows: with a pre-determined static topology of a HVSN, the instantaneous transmission rate on each link and the battery capacity of each wireless node, to maximize the network lifetime by joint optimization of the video encoding rate, the encoding power, and the routing decision as well as the channel contention resolution on each link, subject to the predefined video quality should be satisfied. Mathematically, we can formulate the problem as:

$$\mathbf{P1}: \quad \max_{(\mathbf{f},\mathbf{R},\mathbf{p},\mathbf{T})} \quad [\min_{i\in\mathbb{W}}\{T_i\}] \quad (15)$$

$$\text{s.t.} \quad \sigma^2 e^{-\gamma\cdot R^{(i)}\cdot\left(P_c^{(i)}\right)^{2/3}} \le D_c^{(i)}, \quad \forall i \in \mathbb{W} \quad (16)$$

$$\frac{E^{(i)}}{T_i} = P_c^{(i)} + \sum\nolimits_{l\in\mathcal{O}(i)} (\alpha + \beta\cdot d_l^n)\cdot \frac{f_l}{\tau_l} + c^r \cdot \sum\nolimits_{l\in\mathcal{I}(i)} \frac{f_l}{\tau_l}, \quad \forall i \in \mathbb{W} \quad (17)$$

$$0 \le p_l \le 1, \quad \forall l \in \mathcal{L} \quad (18)$$

$$0 \le P_i \le 1, \quad \forall i \in \mathbb{W}\bigcup\mathbb{P} \quad (19)$$

$$f_l \ge 0, \quad \forall l \in \mathcal{L} \quad (20)$$

$$R^{(i)} \ge 0, \quad \forall i \in \mathbb{W} \quad (21)$$

along with (3) - (6) and (9). Constraint (16) represents that the encoding distortion should not exceed the corresponding upper bound on each wireless node. Constraint (17) reflects the power consumption of each wireless video sensor node. By observation, variables $P_c^{(i)}$, τ_l and P_i are dummy variables since these can be determined in expressions of other variables. Hence, the optimization variables in $\mathbf{P1}$ are $f_l, R^{(i)}$, p_l and T_i.

IV. Optimization Approach and Distributed Algorithm

The problem in $\mathbf{P1}$ is not convex due to non-linearity in constraints (4) and (17). In order to convert the problem to a convex problem, we reformulate constraint (4) by taking the logarithm on both sides. Also, variable $q_i = 1/T_i$ is introduced in (17) as node i's normalized power consumption regarding to its battery capacity $E^{(i)}$. Hence, the objective function becomes $\max(\min_{i\in\mathbb{W}}\{T_i\}) = \min(\max_{i\in\mathbb{W}}\{q_i\})$. Also, (16) is simplified by taking the logarithm on both sides. In addition, $F_l = f_l/\tau_l$ is introduced as the total information flow rate on each link.

The objective function, $\max_{i\in\mathbb{W}}\{q_i\}$, however, is non-differentiable and needs all sensor nodes' information. Hence, it is difficult to develop a fully distributed algorithm to solve the problem.

$$\max_{i\in\mathbb{W}} q_i = \| q \|_\infty = \lim_{k\to+\infty} \| q \|_k = \lim_{k\to+\infty} \left(\sum_{i\in\mathbb{W}} q_i^k\right)^{\frac{1}{k}} \quad (22)$$

In (22), we approximate the max-norm, $\| q \|_\infty$, by the k-norm [17], $\| q \|_k$, where k is a sufficiently large integer. However, the objective function are not strictly convex regarding to F_l and $R^{(i)}$, respectively. Consequently, the resulting dual function would be non-differentiable. Hence, the optimal results of F_l and $R^{(i)}$ can not be obtained directly. This however can be solved by adding a quadratic regularization term [18] for each F_l and $R^{(i)}$ in order to transform the original function into strictly convex. Furthermore, the objective function $\| q \|_k$ can be slightly changed to $\| q \|_k^k$, therefore, the optimization problem in $\mathbf{P1}$ becomes

$$\mathbf{P2}: \quad \min_{(\mathbf{F},\mathbf{R},\mathbf{p},\mathbf{q})} \quad \left[\sum_{i\in\mathbb{W}} q_i^k + \sum_{i\in\mathbb{W}} \delta\cdot\left(R^{(i)}\right)^2 + \sum_{l\in\mathcal{L}} \delta\cdot(F_l)^2\right] \quad (23)$$

$$\text{s.t.} \quad \sum\nolimits_{l\in\mathcal{O}(i)} F_l\cdot\tau_l - \sum\nolimits_{l\in\mathcal{I}(i)} F_l\cdot\tau_l = R^{(i)}, \forall i\in\mathbb{W}\bigcup\mathbb{P} \quad (24)$$

$$\frac{1}{\gamma\cdot\left(P_c^{(i)}\right)^{2/3}}\cdot\ln\left(\frac{\sigma^2}{D_c^{(i)}}\right) \le R^{(i)}, \quad \forall i\in\mathbb{W} \quad (25)$$

$$F_l \le C_l^0, \quad \forall l\in\mathcal{L} \quad (26)$$

$$E^{(i)}\cdot q_i = P_c^{(i)} + \sum\nolimits_{l\in\mathcal{O}(i)}(\alpha+\beta\cdot d_l^n)\cdot F_l + c^r\cdot\sum\nolimits_{l\in\mathcal{I}(i)} F_l, \quad \forall i\in\mathbb{W} \quad (27)$$

$$\ln\tau_l = \ln(1-\varepsilon_l)\cdot p_l + \sum\nolimits_{k\in N_l^I}\ln(1-P_k), \quad \forall l\in\mathcal{L} \quad (28)$$

$$F_l \ge 0, \quad \forall l\in\mathcal{L} \quad (29)$$

along with (3), (17) - (19) and (21). The optimization variables are $F_l, R^{(i)}$, p_l and q_i. δ ($\delta > 0$) represents the regularization factor. If we take a very small value of δ, the result of the objective function in $\mathbf{P2}$ should be close to the objective value in $\mathbf{P1}$. In $\mathbf{P2}$, it can be proved that the objective function is strictly convex, the equality constraints are affine, and the inequality constraints are convex. Hence, they are convex optimization problems [19].

It can be proved that [17] the normalized power consumption q obtained by solving problem $\mathbf{P2}$ can well approximate the one obtained by solving problem $\mathbf{P1}$ given k to be a sufficiently large integer. Hence, problem $\mathbf{P2}$ is effectively equal to problem $\mathbf{P1}$, but the solution can be obtained easier in a fully distributed manner.

To develop a distributed algorithm for $\mathbf{P2}$, the primal decomposition method [20] is used regarding the coupling variable F_l, which results in a two-level optimization problem,

$$\mathbf{P2a}: \quad \min_{(\mathbf{R},\mathbf{p},\mathbf{q})} \quad \left[\sum_{i\in\mathbb{W}} q_i^k + \sum_{i\in\mathbb{W}}\delta\cdot\left(R^{(i)}\right)^2\right] \quad (30)$$

along with (3), (17) - (19), (21), (24), (25), (27) and (28).

$$\mathbf{P2b}: \quad \min_{(\mathbf{F})} \quad \left[U^*(\mathbf{F}) + \sum_{l\in\mathcal{L}}\delta\cdot(F_l)^2\right] \quad (31)$$

along with (26) and (29). Problem $\mathbf{P2a}$ updates the low-level optimization given the $F_l = f_l/\tau_l$ is determined. F_l is determined in the high-level optimization problem $\mathbf{P2b}$. $U^*(\mathbf{F})$ represents the optimal value of the objective function in $\mathbf{P2a}$ with fixed variables, F_l.

Further steps in solving problems $\mathbf{P2a}$ and $\mathbf{P2b}$ involve performing dual decomposition [20] regarding to constraints (24) and (25) in $\mathbf{P2a}$ and constraint (26) in $\mathbf{P2b}$, and formulating the Lagrangian, respectively. The problems can then be solved by the subgradient algorithm. Here, we only show the results and the details are omitted due to space limitation.

1) Low-Level Optimization Problem $\mathbf{P2a}$*:*

$$\lambda_i(n_L+1) = \lambda_i(n_L) + \omega(n_L)\cdot\left(\sum\nolimits_{l\in\mathcal{O}(i)} F_l\cdot\tau_l - \sum\nolimits_{l\in\mathcal{I}(i)} F_l\cdot\tau_l - R^{(i)}\right) \quad (32)$$

$$\theta_i(n_L+1) = \{\theta_i(n_L) + \omega(n_L)\cdot[\frac{1}{\gamma\cdot\left(P_c^{(i)}\right)^{\frac{2}{3}}}\cdot\ln(\frac{\sigma^2}{D_c^{(i)}}) - R^{(i)}]\}^+ \quad (33)$$

where λ and θ are Lagrange multipliers regarding to constraints (24) and (25) in $\mathbf{P2a}$, respectively. n_L represents the low-level iteration index, $\{x\}^+$ represents the maximum of 0 and x, and $\omega(n_L)$ is a positive step size.

Update of q (application layer):

$$q_i(n_L+1) = \{q_i(n_L) - \omega(n_L)\cdot[k\cdot q_i^{k-1} - \frac{2}{3}\cdot\theta_i\cdot\frac{\ln\left(\frac{\sigma^2}{D_c^{(i)}}\right)}{\gamma}\cdot\left(P_c^{(i)}\right)^{-5/3}\cdot E^{(i)}]\}^+ \quad (34)$$

where $P_c^{(i)}$ can be obtained as

$$P_c^{(i)} = E^{(i)}\cdot q_i - \sum\nolimits_{l\in\mathcal{O}(i)}(\alpha+\beta\cdot d_l^n)\cdot F_l - c^r\cdot\sum\nolimits_{l\in\mathcal{I}(i)} F_l \quad (35)$$

Source rate (application layer):

$$R^{(i)} = \{\frac{\lambda_i+\theta_i}{2\cdot\delta}\}^+ \quad (36)$$

Transmission attempt probability (MAC layer):

$$p_l = \begin{cases} \frac{F_l \cdot (\lambda_{\mathcal{I}^{-1}(l)} - \lambda_{\mathcal{O}^{-1}(l)})}{\mu_i} & , \quad \mu_i \neq 0 \\ \frac{1}{|\mathcal{O}(i)|+|L^{\mathcal{I}}(i)|} & , \quad \mu_i = 0 \end{cases} \tag{37}$$

where μ_i can be obtained as

$$\begin{aligned} \mu_i = & \sum\nolimits_{l \in \mathcal{O}(i)} F_l \cdot (\lambda_{\mathcal{I}^{-1}(l)} - \lambda_{\mathcal{O}^{-1}(l)}) \\ & + \sum\nolimits_{k \in L^{\mathcal{I}}(i)} F_k \cdot (\lambda_{\mathcal{I}^{-1}(k)} - \lambda_{\mathcal{O}^{-1}(k)}) \end{aligned} \tag{38}$$

where $\mathcal{O}^{-1}(l)$ denotes the node regarding to the outgoing link l, $\mathcal{I}^{-1}(l)$ denotes the node regarding to the incoming link l, and $L^{\mathcal{I}}(i)$ represents the set of links whose transmission would be interfered by the transmission of node i.

2) High-Level Optimization Problem $\mathbf{P2b}$*:* It is aimed to find the routing and link capacity allocation in this level of the optimization problem. Suppose $\hat{\tau}_l$, $\hat{\lambda}_{O^{-1}(l)}$ and $\hat{\lambda}_{I^{-1}(l)}$ are the optimal variable and Lagrange price corresponding to constraint (24) in problem $\mathbf{P2a}$.

Actual physical flow rate (network layer):

$$F_l = \{\frac{\hat{\tau}_l \cdot (\hat{\lambda}_{\mathcal{I}^{-1}(l)} - \hat{\lambda}_{\mathcal{O}^{-1}(l)}) - \varphi_l}{2 \cdot \delta}\}^+ \tag{39}$$

and the Lagrangian dual variable corresponding to (26) is updated as

$$\varphi_l(n_H + 1) = \{\varphi_l(n_H) + \varpi(n_H) \cdot (F_l - C_l^0)\}^+ \tag{40}$$

where n_H and $\varpi(n_H)$ denote the iteration index and the positive step size in $\mathbf{P2b}$, respectively.

In the proposed algorithm, computation related to each link $l = (i, j)$ is assigned to the transmission node i, and the algorithm only requires information exchange with the neighboring nodes. Therefore, the proposed algorithm is fully distributed.

V. Numerical Results

The performance of the proposed distributed algorithm will be evaluated in this section. The topology used for the HVSN is shown in Fig. 1, where nodes 1-3 and node 5 (sink node) are located at four corners of a square area of 20 m $\times$ 20 m. Node 4 is placed at the center of the square area. Nodes 1-3 are wireless nodes, while nodes 4 and 5 are PL nodes. For performance comparison, we also consider two WVSN topologies: a) same as Fig. 1 except that all nodes are wireless nodes, b) same as the topology in a) except that node 4 is removed. In the following, the topologies in a) and b) are referred to as 5-node and 4-node WVSNs, respectively. The wireless nodes can communicate with all the other nodes within its transmission distance through wireless links, while the PL node can communicate with all the other nodes through wireless links or to the other PL nodes through PL links. The numerical values of all parameters are summarised in Table I. Also, the required maximum encoding distortion $D_c^{(i)}$ in mean-square-error (MSE) is set to 100 if not specified otherwise. The regularization factor is set to $\delta = 0.02$. α is set to 0.2 J/Mb. β, is set to 1.3×10^{-8} $J/Mb/m^4$ and c^r is set to 0.1 J/Mb.

TABLE I. Details of Model Parameters in the HVSN

Parameter	Description	Value
σ^2	Input variance of the video in MSE	3500
γ	Encoding efficiency coefficient	5 $W^{3/2}/Mb/s$
$E^{(i)}$	Initial battery capacity at wireless node i	2 MJ
f_w	Radio frequency	900 MHz
$\overline{p}_{l_w}$	Transmission power of wireless link	0.5 W
$\overline{B}_{l_w}$	Transmission bandwidth of wireless link	1 MHz
N_{l_w}	Noise PSD level of wireless link	-131 dBm/Hz
f_p	Carrier frequency of PL link	110 kHz
$\overline{p}_{l_p}$	Transmission power of PL link	-25 dBm/Hz
$\overline{B}_{l_p}$	Transmission bandwidth of PL link	0.05 MHz
N_{l_p}	Noise PSD level of PL link	-80 dBm/Hz
BER	Target BER	10^{-4}
n	Wireless path loss exponent	4
ε_l	Packet loss rate at link l	0.1

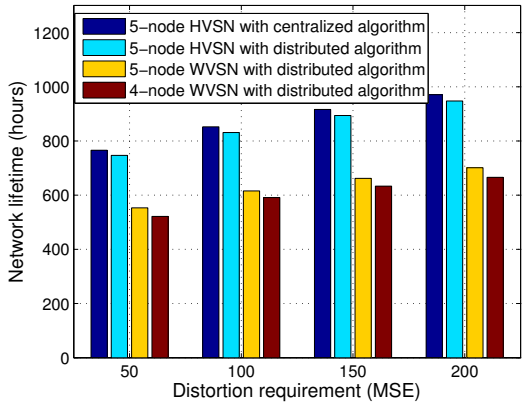

Fig. 2. Comparison of the network lifetime under different distortion requirements

A. Performance Comparison with Centralized Algorithm

In order to obtain the simulation results, a fixed step size of 0.008 is used for both levels of the optimization update and k is set to 10 in the simulation. The maximum network lifetime solved by the centralized algorithm is 851.94 hours, while the network lifetime obtained from the proposed algorithm is 831.11 hours (shown in Fig. 2 with distortion requirement equal to 100). We see that a small performance loss is incurred in the distributed algorithm as compared to the centralized algorithm as a regularization factor is introduced for the development of the distributed algorithm. As shown in Fig. 2, when the regularization factor is 0.02, the network lifetime obtained from the distributed algorithm is sacrificed by around 2.5% compared to the centralized algorithm under different distortion requirements.

B. Comparison of Network Lifetime

Fig. 2 depicts that the network lifetime of the HVSN is increased by around 35% and 42%, respectively, when compared to the 5-node WVSN and 4-node WVSN under different distortion requirements. This is mainly because that with the deployment of the PL node, the total throughput of the network is increased (PL channel capacity) and the communication range of the wireless links are decreased (wireless nodes transmit its data to the PL node instead of to the destination directly) thus saving the energy.

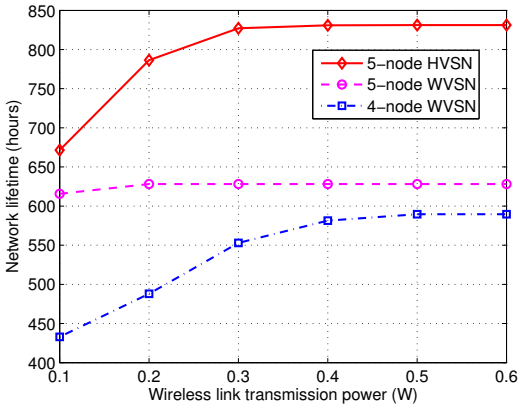

Fig. 3. Comparison of the network lifetime for HVSN with WVSNs with different power for wireless links

TABLE II. COMPARISON OF POWER CONSUMPTION IN THE HVSN

	Tx. power = 0.1 W	Tx. power = 0.5 W
Encoding power (W)	0.61	0.35
Communication power (W)	0.22	0.32
Total power consumption (W)	0.83	0.67

Fig. 3 depicts the effect of transmission power of wireless links on the normalized network lifetime. It is shown that, beyond a certain threshold of the transmission power (*e.g.*, 0.5 W for the HVSN in Fig. 3), the normalized network lifetime remains the same. This is because when the transmission power is low, the wireless channel cannot support sufficient channel capacity, each sensor node would then consume a majority of its power consumption for encoding (as shown in Table II), which results in a low source rate (note a certain distortion requirement can be achieved by either increasing the encoding power or the encoding source rate). While beyond a certain threshold, with further increase in the transmission power, while the channel capacity increases, each node does not encode the video content with the maximum source rate supported by the channel capacity. This is because while encoding the video content with maximum achievable source rate can decrease the encoding power, however, each node would consume more power for data transmission and reception.

VI. CONCLUSION

We have developed a distributed algorithm for network lifetime maximization in a HVSN. Each node solves the optimization problem locally and only requires information exchange with its neighboring nodes. The performance of the proposed algorithm is evaluated through numerical simulations. The results demonstrated that the network lifetime obtained by the proposed distributed algorithm is very close to the one achieved by the centralized algorithm. Also, the investigated 5-node HVSN can achieve 35% and 42% increase in the network lifetime, respectively, as compared to the 5-node WVSN and 4-node WVSN. Future work includes the study of the impacts of dynamic network change, network scale and packet loss rate on the performance of the proposed algorithm. In addition, the current work has focused on the static network configuration where the channel is assumed to be the same throughout the whole lifetime. However, in a home video sensor network scenario, the wireless and PL channels exhibit time-varying and frequency-selective characteristics. It would be worthwhile to develop an algorithm taking the impact of these characteristics of the communication channels into account in future study.

REFERENCES

[1] Z. He and D. Wu, "Resource allocation and performance analysis of wireless video sensors," *IEEE Trans. Circuits Syst. Video Tech.*, vol. 16, no. 5, pp. 590–599, 2006.

[2] L. Gasparini, R. Manduchi, M. Gottardi, and D. Petri, "An ultralow-power wireless camera node: Development and performance analysis," *IEEE Trans. Instrument. Measure.*, vol. 60, no. 12, pp. 3824–3832, 2011.

[3] https://www.arlo.com/.

[4] http://www.logitech.com/en-gb/product/circle/.

[5] H. Wang, N. Agoulmine, M. Ma, and Y. Jin, "Network lifetime optimization in wireless sensor networks," *IEEE J. Sel. Areas Commun.*, vol. 28, no. 7, pp. 1127–1137, 2010.

[6] H. Yetgin, K. T. K. Cheung, M. El-Hajjar, and L. Hanzo, "Cross-layer network lifetime maximization in interference-limited WSNs," *IEEE Trans. Veh. Tech.*, vol. 64, no. 8, pp. 3795–3803, 2015.

[7] K. Zhu and X. Zhu, "Cross-layer network lifetime maximization for hybrid sensor networks," in *Proc. 2014 IEEE SmartGridComm*, Venice, Italy, Nov. 2014, pp. 404–409.

[8] Y. He, I. Lee, and L. Guan, "Distributed algorithms for network lifetime maximization in wireless visual sensor networks," *IEEE Trans. Circuits Syst. Video Tech.*, vol. 19, no. 5, pp. 704–718, 2009.

[9] J. Zou, H. Xiong, C. Li, R. Zhang, and Z. He, "Lifetime and distortion optimization with joint source/channel rate adaptation and network coding-based error control in wireless video sensor networks," *IEEE Trans. Veh. Tech.*, vol. 60, no. 3, pp. 1182–1194, 2011.

[10] C. Li, J. Zou, H. Xiong, and C. W. Chen, "Joint coding/routing optimization for distributed video sources in wireless visual sensor networks," *IEEE Trans. Circuits Syst. Video Tech.*, vol. 21, no. 2, pp. 141–155, 2011.

[11] N. Yang, I. Demirkol, and W. Heinzelman, "Motion sensor and camera placement design for in-home wireless video monitoring systems," in *Proc. 2011 IEEE Globecom*, Houston, Texas, USA, Dec. 2011, pp. 1–5.

[12] K. Stuhlmuller, N. Farber, M. Link, and B. Girod, "Analysis of video transmission over lossy channels," *IEEE J. Sel. Areas Commun.*, vol. 18, no. 6, pp. 1012–1032, 2000.

[13] S. Pudlewski, N. Cen, Z. Guan, and T. Melodia, "Video transmission over lossy wireless networks: a cross-layer perspective," *IEEE J. Sel. Top. Sign. Proces.*, vol. 9, no. 1, pp. 6–21, 2015.

[14] J. S. Seybold, *Introduction to RF propagation*. John Wiley & Sons, 2005.

[15] http://www.plc.uma.es/channels.htm/.

[16] A. Goldsmith, *Wireless communications*. Cambridge university press, 2005.

[17] R. Madan, Z.-Q. Luo, and S. Lall, "A distributed algorithm with linear convergence for maximum lifetime routing in wireless networks," in *Proc. of the Allerton Conference on Communication, Control, and Computing*, Monticello, Illinois, USA, Sep. 2005.

[18] D. P. Bertsekas and J. N. Tsitsiklis, *Parallel and distributed computation: numerical methods*. Prentice Hall Englewood Cliffs, NJ, 1989, vol. 23.

[19] S. Boyd and L. Vandenberghe, *Convex optimization*. Cambridge university press, 2004.

[20] D. Palomar and M. Chiang, "A tutorial on decomposition methods and distributed network resource allocation," *IEEE J. Sel. Areas Commun*, vol. 24, no. 8, pp. 1439–1451, 2006.